Zinc and Cadmium Tropocoronand Complexes: Effect of Metal Ion Radius on Macrocyclic Ligand Twist and Fold

Linda H. Doerrer and Stephen J. Lippard*

Department of Chemistry, Massachusetts Institute of Technology, Cambridge, Massachusetts 02139

Received January 10, 1997[⊗]

The four-coordinate [Zn(TC-*n*,*m*)], $n + m = 7$, 8, 9, 10, and 12, and [Cd(TC-*n*,*m*)], $n + m = 8$, 9, 10, 12, complexes and the five-coordinate complex [Zn(py)(TC-3,3)] were synthesized and characterized by ^{1}H NMR and UV−vis spectroscopy as well as by X-ray crystallography. The dihedral angle Θ between five-membered N−M−N chelate ring planes increases monotonically as a function of the number of methylene linker units, $n + m$. The Θ angles range from 36.4° in [Zn(TC-3,4)] to 84.7° in [Zn(TC-6,6)] and from 36.5° in [Cd(TC-4,4)] to 78.9° in [Cd(TC-6,6)]. For a given value of $n + m$, a larger dihedral angle is observed in the [M(TC-*n*,*m*)] complex having the smaller metal ion radius. Although changes in Θ largely reflect a twisting motion of the two halves of the macrocycle with respect to one another, in [Cd(TC-4,4)] and [Zn(py)(TC-3,3)] the tropocoronand ligand folds in order to accommodate the metal ion, which is too large to fit into the hole of the macrocycle. Cyclic voltammetric studies in THF and CH_2Cl_2 revealed a window from $-2.25 < E_{1/2} < +0.5$ V vs ferrocenium/ferrocene where the TC-*n*,*m* ligands are not redox active. The structural and electrochemical information afforded by this detailed investigation is essential for interpreting ligand field effects on the physical and chemical properties of tropocoronand complexes of transition metal ions having partially filled d-shells. Crystallographic information: [Zn(py)(TC-3,3)], *C*2/*c*, $a = 19.637(2)$ Å, $b = 8.6418(7)$ Å, $c = 13.5516(11)$ Å, $\beta = 108.598(1)°$, $V = 2179.6(3)$ Å^3, $Z = 4$, $R = 0.0580$, $wR^2 = 0.1036$; [Zn(TC-3,4)], $P2_1/c$, $a = 10.5582(4)$ Å, $b = 8.5280(2)$ Å, $c = 20.1471(8)$ Å, $\beta = 93.587(1)°$, $V = 1810.5(1)$ Å^3, $Z = 4$, $R = 0.0284$, $wR^2 = 0.0663$; [Zn(TC-4,4)], *Fdd*2, $a = 19.012(2)$ Å, $b = 46.316(2)$ Å, $c = 8.517(2)$ Å, $V = 7500(3)$ Å^3, $Z = 16$, $R = 0.0561$, $wR^2 = 0.1444$; [Zn(TC-4,5)], *P*2/*c*, $a = 22.0993(3)$ Å, $b = 9.3733(2)$ Å, $c = 19.9053(2)$ Å, $\beta = 106.552(1)°$, $V = 3952.39(11)$ Å^3, $Z = 8$, $R = 0.0905$, $wR^2 = 0.1811$; [Zn(TC-5,5)], $P6_122$, $a = 10.955(1)$ Å, $c = 30.622(4)$ Å, $V = 3183(1)$ Å^3, $Z = 6$, $R = 0.0593$, $wR^2 = 0.1160$; [Zn(TC-6,6)], $P2_12_12_1$, $a = 10.647(2)$ Å, $b = 11.4171(2)$ Å, $c = 19.027(4)$ Å, $V = 2312.9(8)$ Å^3, $Z = 4$, $R = 0.0473$, $wR^2 = 0.0951$; [Cd(TC-4,4)], $P2_1/c$, $a = 10.2448(9)$ Å, $b = 19.4345(2)$ Å, $c = 9.9038(9)$ Å, $\beta = 101.107(1)°$, $V = 1935.0(3)$ Å^3, $Z = 4$, $R = 0.0675$, $wR^2 = 0.1516$; [Cd(TC-4,5)], $P2_1/n$, $a = 9.6688(5)$ Å, $b = 22.9915(12)$ Å, $c = 10.3002(5)$ Å, $\beta = 117.268(1)°$, $V = 2035.3(2)$ Å^3, $Z = 4$, $R = 0.0778$, $wR^2 = 0.1381$; [Cd(TC-5,5)], *C*2/*c*, $a = 12.9224(4)$ Å, $b = 17.0359(5)$ Å, $c = 9.5653(3)$ Å, $\beta = 97.562(1)°$, $V = 2087.4(4)$ Å^3, $Z = 4$, $R = 0.0203$, $wR^2 = 0.0504$; [Cd(TC-6,6)], $P2_12_12_1$, $a = 11.1429(1)$ Å, $b = 11.5325(2)$ Å, $c = 18.3954(3)$ Å, $V = 2363.91(6)$ Å^3, $Z = 4$, $R = 0.0206$, $wR^2 = 0.0475$.

Introduction

The tropocoronand ligand, H_2TC-*n*,*m*, is a tetraazamacrocycle in which two aminotroponiminate rings are connected to one another through polymethylene linker chains of length *n* and *m*. Independent variation of *n* and *m* in the ligand synthesis has afforded tropocoronand macrocycles with ring sizes from 12 to 32.[1−3] Double deprotonation of the ligand provides a dianionic macrocycle capable of binding divalent transition metal ions to form the neutral complexes, [M(TC-*n*,*m*)].

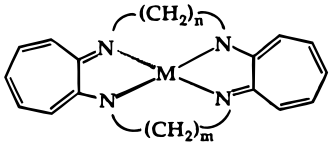

[M(TC-n,m)] tropocoronand

These complexes span the range of four-coordinate geometries.[4−6] The greater the sum $(n + m)$, the more a [M(TC-*n*,*m*)] complex twists from square-planar toward tetrahedral geometry. In the absence of other structural perturbations, increasing the number of methylene units induces torsional strain within each linker chain and destabilizes the complex. To relieve the strain, the two five-membered chelate ring planes twist away from planarity by a dihedral angle Θ, which measures the degree of twist. When Θ is close to 0°, the two tropone rings and four macrocyclic nitrogen atoms form a square-planar metal center. At the other extreme, when Θ approaches 90°, the two aromatic rings are mutually perpendicular and the metal is in a tetrahedral environment. Changing the tropocoronand linker chain lengths gives precise control of Θ and the resulting metal center coordination environment. Previously we described in detail these geometric trends for the mononuclear Co(II),[6] Ni(II),[4] and Cu(II)[5] tropocoronand complexes.

Studies of the Co(II) and Ni(II) complexes further demonstrated that, in addition to the macrocycle ring size, the electronic structure of the transition metal ion could affect the dihedral angle. For example, the TC-4,5 ligand adopts dihedral angles

[⊗] Abstract published in *Advance ACS Abstracts*, May 1, 1997.

(1) Imajo, S.; Nakanishi, K.; Roberts, M.; Lippard, S. J.; Nozoe, T. *J. Am. Chem. Soc.* **1983**, *105*, 2071−2073.
(2) Zask, A.; Gonnella, N.; Nakanishi, K.; Turner, C. J.; Imajo, S.; Nozoe, T. *Inorg. Chem.* **1986**, *25*, 3400−3407.
(3) Shindo, K.; Wakabayashi, H.; Ishikawa, S.; Nozoe, T. *Bull. Chem. Soc. Jpn.* **1993**, *66*, 2941−2948.
(4) Davis, W. M.; Roberts, M. M.; Zask, A.; Nakanishi, K.; Nozoe, T.; Lippard, S. J. *J. Am. Chem. Soc.* **1985**, *107*, 3864−3870.
(5) Davis, W. M.; Zask, A.; Nakanishi, K.; Lippard, S. J. *Inorg. Chem.* **1985**, *24*, 3737−3743.
(6) Jaynes, B. S.; Doerrer, L. H.; Liu, S.; Lippard, S. J. *Inorg. Chem.* **1995**, *34*, 5735−5744.

S0020-1669(97)00033-5 CCC: $14.00

which differ by almost 30° for the Co(II) and Ni(II) complexes.[4,6] The d^7 Co(II) ion has a greater preference for tetrahedral than square-planar geometry compared to d^8 Ni(II), resulting in a larger Θ value for [Co(TC-4,5)]. Differences in ligand field stabilization energies therefore contribute to the larger tropocoronand ligand twist in [Co(TC-4,5)] versus [Ni(TC-4,5)].

In order to delineate more clearly electronic from stereochemical contributions to Θ, we have examined closed-shell systems which permit the study of coordination geometries in the absence of ligand field effects arising from partially filled d-orbitals. In particular, the synthesis and structural characterization of [Zn(TC-*n*,*m*)] complexes were undertaken. We were also interested in understanding the extent to which changing metal ion radii might affect the geometry of metal tropocoronands. Differences in metal ion radii among the late transition metal ions are relatively small,[4−7] making it difficult to distinguish the effects of metal ion size from crystal packing forces. The [Cd(TC-*n*,*m*)] complexes were therefore prepared because the large difference in ionic radii between Zn(II) and Cd(II), 0.2 Å,[7] affords an opportunity to measure accurately the effect of metal ion size on the coordination geometry. In addition to these structural questions, cyclic voltammetric studies of [Zn(TC-*n*,*m*)] complexes were undertaken in order to investigate the redox stability of the tropocoronand ligand. Such knowledge was required in order to interpret the more interesting behavior of the [Co(TC-*n*,*m*)] system.[8]

Experimental Section

General Information. All reactions were carried out in a nitrogen-filled glovebox or by using standard Schlenk techniques. Pentane, toluene, and tetrahydrofuran were distilled from sodium benzophenone ketyl. Methylene chloride and pyridine were distilled from calcium hydride, and acetonitrile was predried with P_2O_5 and then distilled from CaH_2. All solvents were distilled under dinitrogen. Tropocoronand ligands H_2TC-*n*,*m* were prepared as described.[2] The starting materials $[Zn(NCCH_3)_4](BF_4)_2$ and $[Cd(NCCH_3)_6](BF_4)_2$ were prepared by substitution of $ZnCl_2$ or $CdCl_2$ for $CoCl_2$ and $AgBF_4$ for $AgPF_6$ in a literature synthesis for $[Co(NCCH_3)_4](PF_6)_2$.[9] All other reagents were obtained commercially and not purified further. UV−visible spectra were recorded on a Cary 1 E spectrophotometer. ^{1}H NMR spectra were measured on a Bruker AC 250 MHz spectrometer.

Synthetic Procedures. [Zn(py)(TC-3,3)]. A portion of H_2TC-3,3 (101.8 mg, 0.318 mmol) was dissolved in 12 mL of THF, and 2 equiv of *n*-BuLi (0.794 mL, 0.635 mmol of 1.6 M solution in hexanes) was added with vigorous stirring. A deep orange solution was formed which lightened noticeably upon addition of 1 equiv of $[Zn(NCCH_3)_4](BF_4)_2$ (128 mg, 0.318 mmol). Several drops of pyridine were then added. After the solution was stirred for 4 h, the solvents were removed in vacuo and the yellow-orange solid was triturated twice with 2 mL of pentane. The crude product was extracted into 15 mL of CH_2Cl_2, which was filtered through Celite and concentrated to dryness. Dark gold needles (60 mg, 41% yield) suitable for X-ray crystallography were grown from cooling a supersaturated hot toluene solution of the compound to room temperature. ^{1}H NMR (δ, ppm, C_6D_6): 1.72 (m, 4H, C−CH_2−C), 3.35 (m, 8H, N−CH_2−C), 6.31 (m, 4H, H_c/H_b-py), 6.41 (d, J = 11 Hz, 4H, H_a), 7.06 (t, 1H, J = 10 Hz, H_c-py), 7.10 (t, 4H, J = 10 Hz, H_b), 8.04 (d, 2H, J = 6 Hz, H_a-py). UV−vis (THF) [λ_{max}, nm (ϵ_M, M^{-1} cm^{-1})]: 294 (10 300), 389 (35 700), 435 (34 300), 456 (10 900). Anal. Calcd for $ZnN_5C_{25}H_{27}$: C, 64.87; H, 5.88; N, 15.13. Found: C, 64.49; H, 5.84; N, 14.81.

[Zn(TC-3,4)]. A portion of H_2TC-3,4 (61.5 mg, 0.184 mmol) was dissolved in 8 mL of THF and doubly deprotonated with *n*-BuLi (0.230 mL, 0.368 mmol of 1.6 M solution in hexanes). A 1 equiv amount of $[Zn(NCCH_3)_4](BF_4)_2$ (74.1 mg, 0.184 mmol) was added to the deep gold solution which was allowed to stir for 1 h. The solvents were removed in vacuo, the crude product was triturated twice with 3 mL of pentane, and the dark orange product was extracted into CH_2Cl_2 which was filtered through Celite. After removal of CH_2Cl_2 in vacuo, recrystallization from warm toluene gave dark orange needles suitable for X-ray crystallography in 20% yield (15.6 mg). ^{1}H NMR (δ, ppm, C_6D_6): 1.63 (m, 6H, C−CH_2−C), 3.07 (m, 4H, N−CH_2−C), 3.38 (m, 4H, N−CH_2−C), 6.35 (t, J = 9 Hz, 2H, H_c), 6.50 (quart, 4H, H_a), 7.02 (t, J = 11 Hz, 4H, H_b). UV−vis (THF) [λ_{max}, nm (ϵ_M, M^{-1} cm^{-1})]: 296 (11 100), 381 (42 000), 433 (24 800), 455 (14 900). Anal. Calcd for $ZnN_4C_{21}H_{24}$: C, 63.40; H, 6.08; N, 14.08. Found: C, 62.97; H, 5.93; N, 13.92.

[Zn(TC-4,4)]. A portion of H_2TC-4,4 (129.0 mg, 0.370 mmol) was dissolved in 10 mL of THF and twice deprotonated with *n*-BuLi (0.48 mL, 0.768 mmol of 1.6 M solution in hexanes) at −30 °C. A 1 equiv amount of $ZnCl_2$ (55.5 mg, 0.370 mmol) was added to the deep gold solution, and the mixture was allowed to stir for 4 h. The solvent was removed in vacuo and the yellow product extracted into CH_2Cl_2. Layering the concentrated solution with pentane produced 100.4 mg (66% yield) of yellow microcrystalline material. Further recrystallization from hot toluene gave topaz needles suitable for X-ray crystallography. ^{1}H NMR (δ, ppm, C_6D_6): 1.66 (m, 8H, C−CH_2−C), 3.24 (m, 8H, N−CH_2−C), 6.32 (t, J = 9 Hz, 2H, H_c), 6.51 (d, J = 11 Hz, 4H, H_a), 6.96 (t, J = 11 Hz, 4H, H_b). UV−vis (THF) [λ_{max}, nm (ϵ_M, M^{-1} cm^{-1})]: 293 (19 200), 381 (29 000), 433 (16 500), 457 (16 500). Anal. Calcd for $ZnN_4C_{22}H_{26}$: C, 64.16; H, 6.36; N, 13.60. Found: C, 64.23; H, 6.35; N, 13.51.

[Zn(TC-4,5)]. A portion of H_2TC-4,5 (200.0 mg, 0.551 mmol) was dissolved in 10 mL of THF and twice deprotonated with *n*-BuLi (0.69 mL, 1.103 mmol of 1.6 M solution in hexanes) at −30 °C. A 1 equiv amount of $[Zn(NCCH_3)_4](BF_4)_2$ (222.4 mg, 0.551 mmol) was added to the deep gold solution which was allowed to stir for 4 h. The solvents were removed in vacuo, the yellow/orange powder was triturated twice with 3 mL of pentane, and the crude product was extracted into CH_2Cl_2. After filtration through Celite, the solution was concentrated to dryness. Recrystallization from a dilute hot toluene solution gave yellow/orange plates (42.1 mg, 18% yield) which were used for X-ray crystallography. ^{1}H NMR (δ, ppm, C_6D_6): 1.45 (m, 10 H, C−CH_2−C), 2.01 (m, 2 H, C−CH_2−C), 3.28 (m, 8H, N−CH_2−C), 6.32 (t, 2H, H_c), 6.49 (quart, 4H, H_a), 6.99 (m, 4H, H_b). UV−vis (THF) [λ_{max}, nm (ϵ_M, M^{-1} cm^{-1})]: 296 (6700), 381 (23 600), 434 (12 500), 460 (14 700). Anal. Calcd for $ZnN_4C_{23}H_{28}$: C, 64.85; H, 6.63; N, 13.15. Found: C, 64.70; H, 6.55; N, 13.00.

[Zn(TC-5,5)]. A portion of H_2TC-5,5 (106.5 mg, 0.283 mmol) was dissolved in 10 mL of THF and twice deprotonated with *n*-BuLi (0.353 mL, 0.565 mmol of 1.6 M solution in hexanes) at −30 °C. A 1 equiv amount of $ZnCl_2$ (42.4 mg, 0.283 mmol) was added to the yellow solution which was allowed to stir for 4 h. The workup followed a procedure similar to that of [Zn(TC-4,4)]. After slow diffusion of pentane into a toluene solution, 57.3 mg (66% yield) of a yellow microcrystalline material was collected. Crystals suitable for X-ray crystallography were grown from hot toluene. ^{1}H NMR (δ, ppm, C_7D_8): 1.38 (m, 8H, C−CH_2−C), 1.93 (m, 4H, C−CH_2−C), 3.31 (m, 8H, N−CH_2−C), 6.22 (t, J = 9 Hz, 2H, H_c), 6.40 (d, J = 11 Hz, 4H, H_a), 6.95 (t, J = 11 Hz, 4H, H_b). UV−vis (THF) [λ_{max}, nm (ϵ_M, M^{-1} cm^{-1})]: 293 (32 600), 380 (46 400), 436 (18 800), 463 (28 900). Anal. Calcd for $ZnN_4C_{24}H_{30}$: C, 65.53; H, 6.87; N, 12.74. Found: C, 64.94; H, 6.72; N, 12.31.

[Zn(TC-6,6)]. A portion of H_2TC-6,6 (177.0 mg, 0.437 mmol) was dissolved in 10 mL of THF and doubly deprotonated with *n*-BuLi (590 μL, 0.944 mmol of 1.6 M in hexanes) at −30 °C. A 1 equiv amount of $ZnCl_2$ (65.5 mg, 0.437 mmol) was added to the yellow solution which was allowed to stir for 4 h. The workup followed a procedure similar to that for [Zn(TC-4,4)]. Recrystallization from boiling toluene gave deep yellow needles which were suitable for analysis and X-ray crystallography in 21% yield (43.1 mg). ^{1}H NMR (δ, ppm, CD_2Cl_2): 1.19 (m, 16H, C−CH_2−C) 2.05 (m, 8H, C−CH_2−C), 3.59 (m, 8H, N−CH_2−C), 6.08 (t, J = 9 Hz, 2H, H_c), 6.55 (d, J = 11 Hz, 4H, H_a), 6.84 (t, J = 11 Hz, 4H, H_b). UV−vis (THF) [λ_{max}, nm (ϵ_M, M^{-1} cm^{-1})]: 287 (34 600), 383 (44 400), 432 (23 200), 457 (39 200). Anal. Calcd for $ZnN_4C_{26}H_{34}$: C, 66.73; H, 7.32; N, 11.97. Found: C, 67.19; H, 7.54; N, 12.03.

(7) Shannon, R. D. *Acta Crystallogr.* **1976**, *A32*, 751−767.
(8) Doerrer, L. H.; Lippard, S. J. Manuscript in preparation.
(9) Goldstein, A. S.; Drago, R. S. *Inorg. Chem.* **1991**, *30*, 4506−4510.

Table 1. Experimental Details of the X-ray Diffraction Studies of Zinc Tropocoronand Complexes

	[Zn(py)(TC-3,3)]	[Zn(TC-3,4)]	[Zn(TC-4,4)]	[Zn(TC-4,5)]	[Zn(TC-5,5)]	[Zn(TC-6,6)]
formula	$ZnN_5C_{25}H_{27}$	$ZnN_4C_{21}H_{24}$	$ZnN_4C_{22}H_{26}$	$ZnN_4C_{23}H_{28}$	$ZnN_4C_{24}H_{30}$	$ZnN_4C_{26}H_{34}$
fw	462.89	397.83	411.84	425.88	439.90	467.96
cryst syst	monoclinic	monoclinic	orthorhombic	monoclinic	hexagonal	orthorhombic
space group	*C*2/*c*	$P2_1/c$	*Fdd*2	*P*2/*c*	$P6_122$	$P2_12_12_1$
a, Å	19.637(2)	10.5582(4)	19.012(2)	22.0993(3)	10.955(1)	10.647(2)
b, Å	8.6418(7)	8.5280(2)	46.316(2)	9.3733(2)		11.4171(2)
c, Å	13.5516(11)	20.1471(8)	8.517(2)	19.9053(2)	30.622(4)	19.027(4)
β, deg	108.598(1)	93.587(1)		106.552(1)		
V, Å^3	2179.6(3)	1810.5(1)	7500(3)	3952.39(11)	3183(1)	2312.9(8)
Z	4	4	16	8	6	4
ρ_{calcd}, g/cm^3	1.41	1.46	1.46	1.41	1.38	1.34
T, K	188	193	213	188	177.1	197.6
μ(Mo Kα), mm^{-1}	1.149	1.369	1.324	1.259	1.175	1.083
transm coeff	0.733−0.956	0.754−0.896	0.941−1.000	0.697−0.862	0.678−1.000	0.941−1.000
2θ limits, deg	3−56.6	3−46.5	3−50	3−56.6	3−50	3−55
tot. no. of data	6745	7057	2478	24084	1425	3313
no. of unique data	2624	2583	2348	9419	1192	3187
obsd data[a]	2099	2339	2047	6892	790	2283
no. of params	142	235	244	505	133	280
R,[b] %	5.80	2.84	5.61	9.05	5.93	4.73
wR^2,[c] %	10.36	6.63	14.44	18.11	11.60	9.51
largest peak, e/Å^3	0.296	0.252	0.380	2.94[d]	0.389	0.685

[a] Observation criterion: $I > 2\sigma(I)$. [b] $R = \Sigma||F_o| - |F_c||/\Sigma|F_o|$. [c] $wR^2 = \{\Sigma[w(F_o^2 - F_c^2)^2]/\Sigma[w(F_o^2)^2]\}^{1/2}$. [d] The crystals of this compound tend to grow as twins or multiplets showing systematic absence violations, large *R*-factors, and varying amounts of residual electron density in the final difference Fourier maps. The results reported here are among the best obtained for over 10 specimens examined and should be viewed with caution.

[Cd(TC-4,4)]. A portion of H_2TC-4,4 (155.1 mg, 0.445 mmol) was dissolved in 10 mL of THF and doubly deprotonated with *n*-BuLi (556 μL, 0.890 mmol of 1.6 M in hexanes) at −30 °C. A 1 equiv amount of $[Cd(NCCH_3)_6](BF_4)_2$ (237 mg, 0.445 mmol) was added to the yellow solution which was allowed to stir for 4 h. The workup followed a procedure similar to that for [Zn(TC-4,4)]. Recrystallization from toluene gave dark orange rods in 26% yield (53.8 mg) which were suitable for analysis and X-ray crystallography. ^{1}H NMR (δ, ppm, C_6D_6): 1.61 (m, 8H, C−CH_2−C), 3.00 (m, 8H, N−CH_2−C), 6.34 (t, J = 9 Hz, 2H, H_c), 6.47 (d, J = 11 Hz, 4H, H_a), 7.03 (t, J = 11 Hz, 4H, H_b). UV−vis (CH_2Cl_2) [λ_{max}, nm (ϵ_M, M^{-1} cm^{-1})]: 290 (3506), 386 (38 100), 435 (19 500), 461 (18 000). Anal. Calcd for $CdN_4C_{22}H_{26}$: C, 57.58; H, 5.71; N, 12.21. Found: C, 57.17; H, 5.77; N, 11.97.

[Cd(TC-4,5)]. A portion of H_2TC-4,5 (149.3 mg, 0.412 mmol) was dissolved in 10 mL of THF and doubly deprotonated with *n*-BuLi (515 μL, 0.823 mmol of 1.6 M in hexanes) at −30 °C. A 1 equiv amount of $[Cd(NCCH_3)_6](BF_4)_2$ (219 mg, 0.412 mmol) was added to the yellow solution which was allowed to stir for 4 h. The workup followed a procedure similar to that for [Zn(TC-4,4)]. Recrystallization from toluene gave dark orange needles in 10.3% yield (20.0 mg) which were suitable for analysis and X-ray crystallography. ^{1}H NMR (δ, ppm, C_6D_6): 1.63 (m, 10H, C−CH_2−C), 3.05 (m, 4H, N−CH_2−C), 3.22 (m, 4H, N−CH_2−C), 6.33 (t, J = 9 Hz, 2H, H_c), 6.43 (quart, J = 11 Hz, 4H, H_a), 7.04 (t, J = 11 Hz, 4H, H_b). UV−vis (CH_2Cl_2) [λ_{max}, nm (ϵ_M, M^{-1} cm^{-1})]: 286 (31 800), 361 (15 900), 381 (21 300), 437 (12 500), 464 (13 500). Anal. Calcd for $CdN_4C_{23}H_{28}$: C, 58.42; H, 5.97; N, 11.85. Found: C, 58.42; H, 5.95; N, 11.57.

[Cd(TC-5,5)]. A portion of H_2TC-5,5 (74.6 mg, 0.198 mmol) was dissolved in 15 mL of THF and doubly deprotonated with *n*-BuLi (248 μL, 0.396 mmol of 1.6 M in hexanes) at −30 °C. A 1 equiv amount of $[Cd(NCCH_3)_6](BF_4)_2$ (105 mg, 0.198 mmol) was added to the yellow solution which was allowed to stir for 4 h. The workup followed a procedure similar to that for [Zn(TC-4,4)]. Recrystallization from toluene gave orange needles in 33% yield (31.8 mg) which were suitable for analysis and X-ray crystallography. ^{1}H NMR (δ, ppm, C_6D_6): 1.37 (m, 12H, C−CH_2−C), 3.24 (m, 8H, N−CH_2−C), 6.31 (t, J = 9 Hz, 2H, H_c), 6.40 (d, J = 11 Hz, 4H, H_a), 7.02 (t, J = 11 Hz, 4H, H_b). UV−vis (CH_2Cl_2) [λ_{max}, nm (ϵ_M, M^{-1} cm^{-1})]: 291 (16 600), 385 (46 000), 440 (18 200), 466 (23 200). Anal. Calcd for $CdN_4C_{24}H_{30}$: C, 59.20; H, 6.21; N, 11.51. Found: C, 59.02; H, 6.03; N, 11.63.

[Cd(TC-6,6)]. A portion of H_2TC-6,6 (96.6 mg, 0.239 mmol) was dissolved in 15 mL of THF and doubly deprotonated with *n*-BuLi (298 μL, 0.477 mmol of 1.6 M in hexanes) at −30 °C. A 1 equiv amount of $[Cd(NCCH_3)_6](BF_4)_2$ (127 mg, 0.234 mmol) was added to the yellow solution which was allowed to stir for 4 h. The workup followed a procedure similar to that for [Zn(TC-4,4)]. Recrystallization from boiling toluene gave deep yellow needles in 28% yield (27.6 mg) which were analytically pure and suitable for X-ray crystallography. ^{1}H NMR (δ, ppm, C_6D_6): 0.98 (m, 4H, C−CH_2−C), 1.17 (m, 4H, C−CH_2−C), 1.44 (m, 4H, C−CH_2−C), 1.91 (m, 4H, C−CH_2−C), 3.46 (m, 8H, N−CH_2−C), 6.26 (t, J = 9 Hz, 2H, H_c), 6.56 (d, J = 11 Hz, 4H, H_a), 6.94 (t, J = 11 Hz, 4H, H_b). UV−vis (CH_2Cl_2) [λ_{max}, nm (ϵ_M, M^{-1} cm^{-1})]: 290 (16 900), 387 (34 700), 437 (19 000), 463 (25 000). Anal. Calcd for $CdN_4C_{26}H_{34}$: C, 60.64; H, 6.65; N, 10.88. Found: C, 60.50; H, 6.71; N, 10.85.

X-ray Crystallography. General Procedures. Single-crystal diffraction data were collected on either an Enraf-Nonius CAD4 four-circle or a Siemens-CCD SMART diffractometer system. The general procedures for data collection and reduction with each instrument follow those reported previously.[10,11] Structures were solved with the direct methods package SIR-92, an updated version of SIR88,[12] and incorporated into the TEXSAN[13] package of programs, which typically afforded positions for the majority of the non-hydrogen atoms. The remaining atoms were found from the resulting difference Fourier maps and refined by full-matrix least squares and Fourier techniques using the SHELXTL-PLUS program package. For acentric space groups, isotropic refinements were performed with both enantiomorphs and the one with the smaller residuals was chosen. Non-hydrogen atoms were refined anisotropically except as noted. In the structure of [Cd(TC-4,5)], the central carbon atoms of the polymethylene linker chains were disordered. A model was introduced in which the two arms were refined as both $(CH_2)_4$ and $(CH_2)_5$ chains, each with a site occupancy of 0.5. All hydrogen atoms were generated at calculated positions and allowed to ride on their corresponding carbon atoms (d_{C-H} = 0.95 Å, $B_H = 1.2B_C$).

Important crystallographic information for each complex including refinement residuals is given in Table 1 for the zinc tropocoronand complexes. The same information is present in Table 2 for the cadmium tropocoronand complexes. Final positional, equivalent isotropic ther-

(10) Carnahan, E. M.; Rardin, R. L.; Bott, S. G.; Lippard, S. J. *Inorg. Chem.* **1992**, *31*, 5193−5201.
(11) Feig, A. L.; Bautista, M. T.; Lippard, S. J. *Inorg. Chem.* **1996**, *35*, 6892−6898.
(12) Burla, M. C.; Camalli, M.; Cascarano, G.; Giacovazzo, C.; Polidori, G.; Spagna, R.; Viterbo, D. *J. Appl. Crystallogr.* **1989**, *22*, 389−393.
(13) *TEXSAN: Single Crystal Analysis Software*, 2.0 ed.; Molecular Structure Corp. Woodlands, TX, 1993.

Table 2. Experimental Details of the X-ray Diffraction Studies of Cadmium Tropocoronand Complexes

	[Cd(TC-4,4)]	[Cd(TC-4,5)]	[Cd(TC-5,5)]	[Cd(TC-6,6)]
formula	$CdN_4C_{22}H_{26}$	$CdN_4C_{23}H_{28}$	$CdN_4C_{24}H_{30}$	$CdN_4C_{26}H_{34}$
fw	458.87	472.89	486.92	514.97
cryst syst	monoclinic	monoclinic	monoclinic	orthorhombic
space group	$P2_1/c$	$P2_1/n$	$C2/c$	$P2_12_12_1$
a, Å	10.2448(9)	9.6688(5)	12.9224(4)	11.1429(1)
b, Å	19.4345(2)	22.9915(12)	17.0359(5)	11.5325(2)
c, Å	9.9038(9)	10.3002(5)	9.5653(3)	18.3954(3)
β, deg	101.107(1)	117.268(1)	97.562(1)	
V, Å^3	1935.0(3)	2035.3(2)	2087.4(4)	2363.91(6)
Z	4	4	4	4
ρ_{calcd}, g/cm^3	1.575	1.543	1.549	1.447
T, K	188	188	188	188
μ(Mo Kα), mm^{-1}	1.143	1.089	1.064	0.944
transm coeff	0.773−0.856	0.692−0.935	0.716−0.907	0.712−0.910
2θ limits, deg	3−46.5	3−56.6	3−46.5	3−46.5
tot. no. of data	7512	12326	4150	9672
no. of unique data	2754	4836	1496	3374
obsd data[a]	2161	3317	1457	3273
no. of params	244	280	133	280
R,[b] %	6.75	7.78	2.03	2.06
wR^2,[c] %	15.16	13.81	5.04	4.75
largest peak, e/Å^3	0.557	0.704	0.356	0.163

[a] Observation criterion: $I > 2\sigma(I)$. [b] $R = \Sigma||F_o| - |F_c||/\Sigma|F_o|$. [c] $wR^2 = \{\Sigma[w(F_o^2 - F_c^2)^2]/\Sigma[w(F_o^2)^2]\}^{1/2}$.

mal, anisotropic temperature parameters, all bond distances and angles, and torsion angles within the tropocoronand linker chains are provided as Supporting Information in Tables S1−S42.

Electrochemistry. Cyclic voltammetric measurements were performed under a nitrogen atmosphere using an EG&G Model 263 potentiostat. A reference electrode consisting of a silver wire in a 0.1 M $AgNO_3$ acetonitrile solution was used[14] for which the ferrocenium/ferrocene potential was +0.20 V in CH_2Cl_2 and +0.10 V in THF. A platinum wire (0.02 in.) was used as an auxiliary electrode, and a 1.75 mm^2 platinum disc, as the working electrode. Solute samples were typically 2 mM in [Zn(TC-*n*,*m*)], and 0.5 M solutions of (n-Bu_4N)(PF_6) were used.

Results

Syntheses. The complexes [Zn(TC-*n*,*m*)], $n + m = 7$, 8, 9, 10, and 12, and [Cd(TC-*n*,*m*)], $n + m = 8$, 9, 10, and 12, were readily prepared from MX_2 and Li_2TC-*n*,*m* followed by extraction of the product into CH_2Cl_2 to remove LiX and recrystallization from toluene. The smallest macrocycles in these series define the lower limit of tropocoronand macrocycle size which can accommodate a four-coordinate complex for each metal. This phenomenon is discussed in detail below.

A toluene-soluble species could not be extracted from the crude reaction mixture of Li_2TC-3,3 and $ZnCl_2$. From THF we obtained a poor quality structure of the five-coordinate [Zn(LiCl)(TC-3,3)]·3THF species with chloride occupying the axial position of a square pyramid.[15] These results suggested that, although the Zn(II) ion was too large to fit in the N_4 plane of TC-3,3, a complex could be obtained by addition of a fifth ligand. As anticipated, a toluene-soluble [Zn(py)(TC-3,3)] complex could be obtained in the reaction of $[Zn(NCCH_3)_4](BF_4)_2$ with Li_2TC-3,3 in the presence of pyridine.

Structural Characterization. Zinc. The structure of [Zn(py)(TC-3,3)] is square-pyramidal (Figure 1), a geometry consistent with other structurally characterized [MX(TC-3,3)] species.[16−18] The zinc atom sits on a crystallographic 2-fold symmetry axis which relates the two aminotroponiminate rings. The metal is displaced from the N_4 plane by 0.57 Å and the ZnN_{py} distance is 2.096(4) Å. The five-membered chelate rings are bent toward one another by 15° in a saddle-type conformation to enforce good overlap between the macrocyclic nitrogen donors and the displaced zinc atom. The average $Zn-N_{TC}$ distance is 2.055(5) Å. Other selected bond distances and angles are listed in Table 3. The structures of the [Zn(TC-*n*,*m*)] complexes for $n + m = 7$, 8, 9, 10, and 12 are also shown in Figure 1. A plot of Θ versus $n + m$ is given in Figure 2, and Θ values for all structurally characterized [M(TC-*n*,*m*)] complexes are listed in Table 4. Selected distances and angles for individual zinc(II) tropocoronands are collected in Table 3 and linker chain torsion angles and deviations from the expected values are compiled in Table S41.

For the [Zn(TC-*n*,*m*)] structures where $n + m > 7$, the dihedral angles increase monotonically with increasing ($n + m$), as evident from Figure 2; Table 4 compares the results with those obtained previously for the Co(II), Ni(II), or Cu(II) analogs. The chief difference between the Zn(II) and the Co(II)/Ni(II) complexes is the discontinuity in the Θ versus ($n + m$) plots for [Co(TC-*n*,*m*)] and [Ni(TC-*n*,*m*)], depicted in Figure 3, arising at the low- to high-spin transition point. The alteration in zinc dihedral angles is continuous with $n + m$, owing to the lack of a similar spin-state change (Figure 2).

The average Zn−N distances in the [Zn(TC-*n*,*m*)] series are 2.02(2) Å for [Zn(TC-3,4)], 1.99(2) Å for [Zn(TC-4,4)], 1.987(12) Å for [Zn(TC-4,5)], 1.991(5) Å for [Zn(TC-5,5)], and 1.981(3) Å for [Zn(TC-6,6)]. For comparison, the average Zn−N distance in the related acyclic complex, $[Zn(Ph_2ati)_2]$, is 1.98(1) Å, where Ph_2ati = *N*,*N*′-diphenylaminotroponiminate.[19,20]

Cadmium. The structures of [Cd(TC-*n*,*m*)], $n + m = 8$, 9, 10, and 12, are shown in Figure 4. Selected distances and angles for the [Cd(TC-*n*,*m*)] series are collected in Table 5, and the ligand torsion angles with deviations from expected values are reported in Table S42. The dihedral angles observed for the [Cd(TC-*n*,*m*)] complexes are depicted in Figure 2 and compared with those of the first-row metals in Table 4. The Θ values for [Cd(TC-*n*,*m*)], $n + m = 9$, 10, and 12, are uniformly smaller than those of their Zn congeners. The crystal structure of [Cd(TC-4,4)] revealed pseudo-square-planar geometry with cadmium lying 0.124 Å out of the best plane defined by the four nitrogen atoms. This displacement is accompanied by a folding of the tropocoronand ligand, similar to that seen in [Zn(py)(TC-3,3)]. The fold suggests that the TC-4,4 ligand is the smallest which can accommodate four-coordinate cadmium and that smaller ligands would afford $[Cd(base)_x(TC\text{-}n,m)]$ complexes, $x = 1$ or 2, analogous to [Zn(py)(TC-3,3)].

The average Cd−N bond length decreases with the increase in $n + m$, exhibiting a trend similar to that in the [Zn(TC-*n*,*m*)] complexes. The average Cd−N distances are 2.24(1) Å for [Cd(TC-4,4)], 2.200(6) Å for [Cd(TC-4,5)], 2.196(1) Å for [Cd(TC-5,5)], and 2.187(5) Å for [Cd(TC-6,6)].

Spectroscopic Properties. The ^{1}H NMR spectra of the Zn and Cd tropocoronands are quite similar to those of the diamagnetic [Ni(TC-*n*,*m*)] complexes reported previously.[4] The aminotroponiminate resonances, atom labels for which are shown in Figure 5, are readily distinguished from one another

(14) Mann, C. K. In *Electroanalytical Chemistry*; Bard, A. J., Ed.; Marcel Dekker: New York, 1969; Vol. 3, p 61.
(15) Doerrer, L. H.; Lippard, S. J. Unpublished results.
(16) Jaynes, B. S.; Ren, T.; Liu, S.; Lippard, S. J. *J. Am. Chem. Soc.* **1992**, *114*, 9670−9671.
(17) Jaynes, B. S.; Ren, T.; Masschelein, A.; Lippard, S. J. *J. Am. Chem. Soc.* **1993**, *115*, 5589−5599.
(18) Scott, M. J.; Lippard, S. J. Unpublished results.
(19) Laing, M. Personal communication.
(20) Laing, M. *Summer Am. Cryst. Assoc. Abstr.* **1976**, 76.

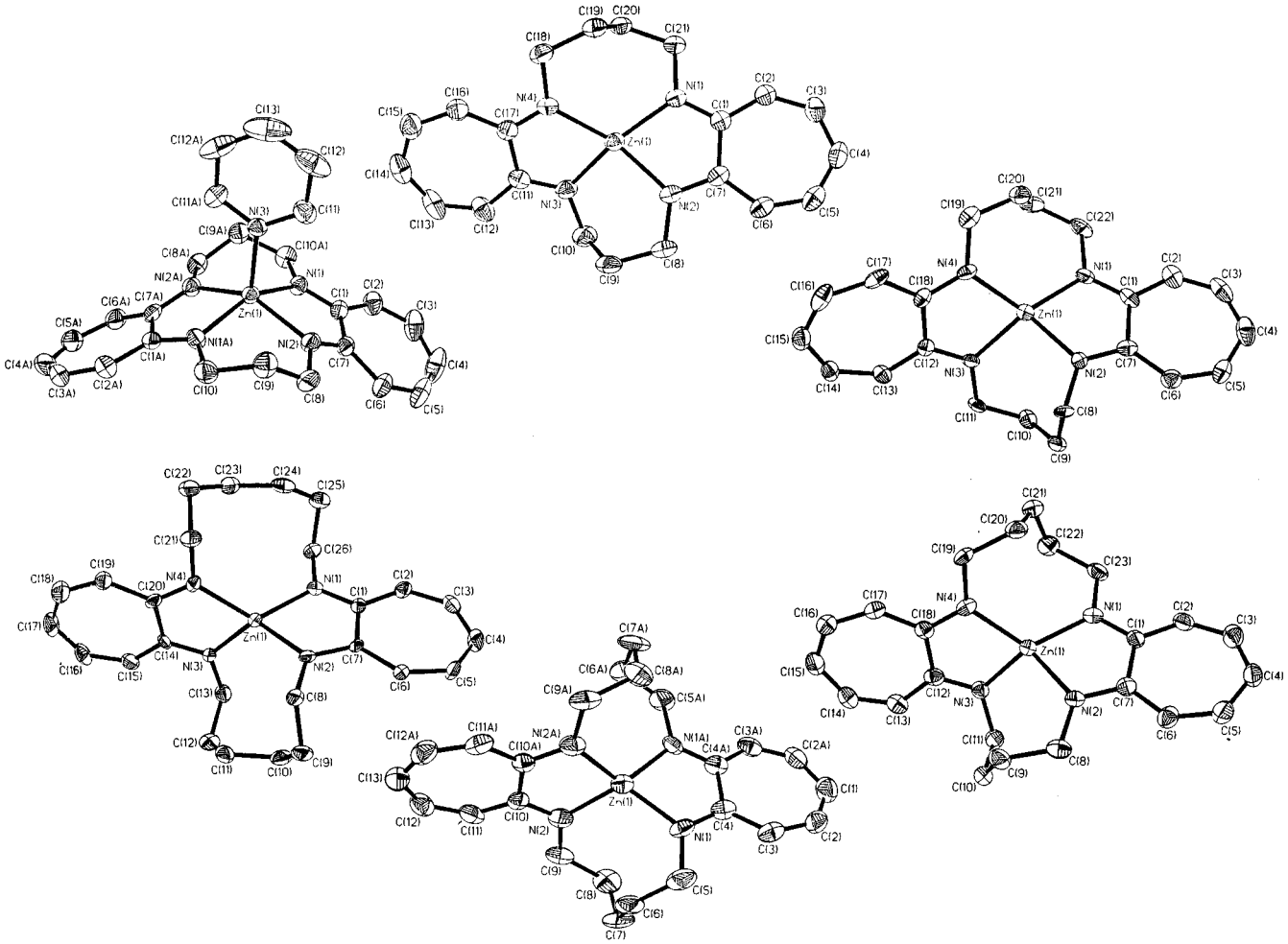

Figure 1. ORTEP diagrams with 50% thermal ellipsoids (clockwise from top left) [Zn(py)(TC-3,3)], [Zn(TC-3,4)], [Zn(TC-4,4)], [Zn(TC-4,5)], [Zn(TC-5,5)], and [Zn(TC-6,6)].

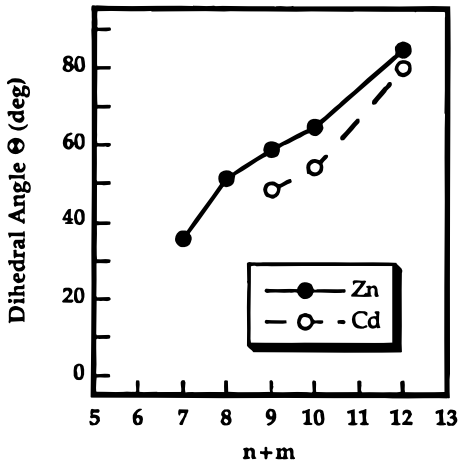

Figure 2. Comparison of [Zn(TC-*n*,*m*)] and [Cd(TC-*n*,*m*)] dihedral angles, Θ, as a function of linker chain length, $(n + m)$.

by the integrated intensities and splitting patterns. The H_a protons appear as a doublet integrating for four protons, and the H_b and H_c protons are present as triplets integrating for four and two protons, respectively. In the asymmetric [M(TC-*n*,*m*)] complexes, the two H_a and H_b protons on the same aminotroponiminate ring are no longer equivalent but appear as two overlapping signals. The ^{1}H NMR spectrum of [Zn(py)(TC-3,3)] displays resonances for bound pyridine distinct from those of the free ligand. Addition of excess pyridine results in only one averaged resonance indicating rapid exchange on the NMR time scale at room temperature.

The UV−vis spectral data show strong intraligand charge transfer bands similar to those reported for other tropocoronand complexes. The only significant change across the series is in relative intensities of the two lowest energy charge transfer bands as the complexes shift from pseudo-square-planar to tetrahedral geometry. In the [Zn(TC-*n*,*m*)] series, the extinction coefficients for the absorbance near 434 nm decrease from 34 300 to 23 200 M^{-1} cm^{-1} in [Zn(py)(TC-3,3)], and those corresponding to the absorbance near 456 nm increase from 10 900 to 39 200 M^{-1} cm^{-1} in [Zn(TC-6,6)]. A similar pattern is present in the [Cd(TC-*n*,*m*)] complexes. The absorption intensity at 435 nm decreases from $\epsilon = 19\,500$ M^{-1} cm^{-1} in [Cd(TC-4,4)] to 19 000 M^{-1} cm^{-1} in [Cd(TC-6,6)] and the extinction coefficient for the 461 nm absorbance increases from 18 000 M^{-1} cm^{-1} in [Cd(TC-4,4)] to 25 000 M^{-1} cm^{-1} in [Cd(TC-6,6)].

Electrochemistry. Cyclic voltammetric studies on [Zn(TC-*n*,*m*)] revealed no reversible redox behavior within the THF solvent window, $0.4 < E° < -3.0$ V. Under more oxidizing potentials in CH_2Cl_2, an irreversible wave was observed at approximately 0.50 V versus ferrocenium/ferrocene. Representative cyclic voltammograms are shown for [Zn(TC-4,4)] in Figure S1 (Supporting Information). All other tropocoronand ligands behaved similarly.

Discussion

Synthesis. Divalent zinc(II) and cadmium(II) TC-*n*,*m* complexes were obtained by the reported procedures in moderate

Table 3. Selected Bond Distances (Å) and Angles (deg) for Zinc Tropocoronands[a]

	distances		angles	
[Zn(py)(TC-3,3)]	Zn−N1	2.050(3)	N1−Zn−N1A	145.0(2)
	Zn−N2	2.060(3)	N1−Z−N2	77.8(1)
	Zn−N3	2.096(4)	N1−Zn−N2A	93.4(1)
	Zn−N_{TCavg}	2.055(5)	N2−Zn−N2A	150.6(2)
			N1−Zn−N3	107.50(8)
			N2−Zn−N3	104.71(8)
[Zn(TC-3,4)]	Zn−N1	1.998(2)	N1−Zn−N2	79.86(8)
	Zn−N2	2.045(2)	N1−Zn−N3	155.22(8)
	Zn−N3	2.003(2)	N1−Zn−N4	115.47(8)
	Zn−N4	2.027(2)	N2−Zn−N3	94.77(8)
	Zn−N_{avg}	2.02(2)	N2−Zn−N4	153.74(8)
			N3−Zn−N4	79.44(8)
[Zn(TC-4,4)]	Zn−N1	1.986(7)	N1−Zn−N2	80.5(3)
	Zn−N2	1.983(7)	N1−Zn−N3	151.1(3)
	Zn−N3	2.022(7)	N1−Zn−N4	117.4(3)
	Zn−N4	1.982(7)	N2−Zn−N3	99.0(3)
	Zn−N_{avg}	1.99(2)	N2−Zn−N4	141.4(3)
			N3−Zn−N4	80.9(3)
[Zn(TC-4,5)][b]	Zn1−N1	1.974(5)	N1−Zn1−N2	81.8(2)
	Zn1−N2	1.995(5)	N1−Zn1−N3	141.0(2)
	Zn1−N3	1.985(5)	N1−Zn1−N4	120.2(2)
	Zn1−N4	1.991(5)	N1B−Zn1B−N2B	81.4(2)
	Zn1B−N1B	1.995(5)	N1B−Zn1B−N3B	142.4(2)
	Zn1B−N2B	1.970(5)	N1B−Zn1B−N4B	120.5(2)
	Zn1B−N3B	2.009(5)	N2−Zn1−N3	102.2(2)
	Zn1B−N4B	1.975(4)	N2−Zn1−N4	140.5(2)
	Zn−N_{avg}	1.987(12)	N3−Zn1−N4	81.1(2)
			N2B−Zn1B−N3B	101.2(2)
			N2B−Zn1B−N2B	140.6(2)
			N3B−Zn1B−N4B	81.0(2)
[Zn(TC-5,5)]	Zn−N1	1.985(7)	N1−Zn−N1A	81.3(5)
	Zn−N2	1.996(8)	N1−Zn−N2	115.3(3)
	Zn−N_{avg}	1.991(5)	N1−Zn−N2A	135.8(3)
			N2−Zn−N2A	82.2(5)
Zn(TC-6,6)]	Zn−N1	1.984(5)	N1−Zn−N2	81.3(2)
	Zn−N2	1.984(5)	N1−Zn−N3	125.2(2)
	Zn−N3	1.972(5)	N1−Zn−N4	123.3(2)
	Zn−N4	1.982(5)	N2−Zn−N3	121.4(2)
	Zn−N_{avg}	1.981(3)	N2−Zn−N4	130.8(2)
			N3−Zn−N4	81.1(2)

[a] Numbers in parentheses are estimated standard deviations of the last significant figure. Atoms are labeled as indicated in Figure 1.[b] See footnote *d*, Table 1.

Table 4. Dihedral Angles for [M(TC-*n*,*m*)] Complexes

	Θ (deg) for [M(TC-*n*,*m*)]				
$n + m$	Co[a] (0.72 Å)[b]	Ni[c] (0.69 Å)	Cu[d] (0.71 Å)	Zn (0.74 Å)	Cd (0.92 Å)
6	9.0	8.3	0.0	*e*	*e*
7	*f*	*f*	*f*	36.4	*e*
8	31.8	28.9	36.6	51.1	*g*
9	58.7	27.1	*f*	59.7	48.5
10	69.9	70.1	61.3	70.2	54.9
12	84.5	85.2	*e*	84.7	78.9

[a] Reference 6. [b] Ionic radius, ref 7. [c] Reference 4. [d] Reference 5. [e] Complex not accessible. [f] Structure not determined. [g] See discussion for [Cd(TC-4,4)] in text.

yields. The two series of compounds differ primarily in their solubility, the latter being notably less soluble in solvents such as toluene and fluorobenzene. Although the complexes are stable for short periods of time in the solid state in air, yellow-gold solutions of [M(TC-*n*,*m*)], M = Zn, and Cd, and crystals in mother liquor decompose in the atmosphere to dark brown heterogeneous mixtures in a few hours. Although the nature of the decomposition products was not investigated, it is possible that hydrolysis occurred to afford H_2TC-*n*,*m* and the metal hydroxide/oxide.

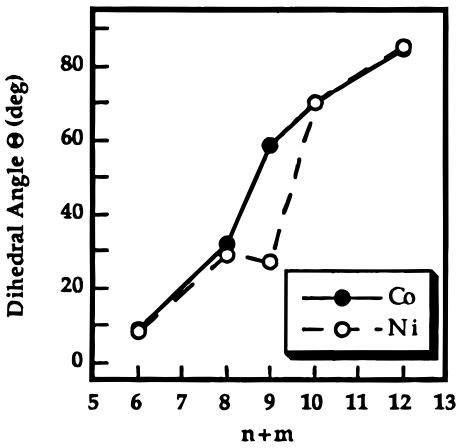

Figure 3. Comparison of [Co(TC-*n*,*m*)] and [Ni(TC-*n*,*m*)] dihedral angles as a function of linker chain length, ($n + m$).

Structural Properties. [Zn(TC-*n*,*m*)] Complexes. Most structurally characterized zinc(II) complexes have either square-planar or tetrahedral geometry. Since Zn(II) has no geometric preferences based on its d^{10} electronic structure, the structures are determined solely by the steric demands of the ligands. Most of the structurally characterized square-planar ZnN_4 complexes are Zn(II) porphyrins,[21−25] although porphycene analogs have also been prepared.[26] Most other structurally characterized four-coordinate ZnN_4 complexes have essentially tetrahedral geometries.[27−32] A few macrocyclic tetrahedral complexes are known, such as those with triazacyclononane,[33] but the majority of tetrahedral ZnN_4 complexes have acyclic ligands. A rare structurally characterized example of a ZnN_4 complex with a geometry intermediate between square-planar and tetrahedral is [Zn(Ph_2ati)$_2$], in which the dihedral angle between the two chelate rings is 66.5°.[19,20] This structure seems to be determined by the geometry required for minimizing the interaction between the bulky phenyl substituents.

The [Zn(TC-*n*,*m*)] complexes nicely demonstrate the tuning potential of the tropocoronand macrocycle by affording several members with geometries between square-planar and tetrahedral. A rigorously square-planar four-coordinate complex was not obtained, however. Extrapolation of the plot (Figure 2) of Θ versus $n + m$ for [Zn(TC-*n*,*m*)] to the $n + m = 6$ point predicts a dihedral angle of approximately 25°. This value would require a remarkable distortion of the TC-3,3 ligand, for which a twist

(21) Scheidt, W. R.; Kastner, M. E.; Hatano, K. *Inorg. Chem.* **1978**, *17*, 706−710.
(22) Senge, M. O.; Eigenbrot, C. W.; Brennan, T. D.; Shusta, J.; Scheidt, W. R.; Smith, K. M. *Inorg. Chem.* **1993**, *32*, 3134−3142.
(23) Byrn, M. P.; Curtis, C. J.; Khan, S. I.; Sawin, P. A.; Tsurumi, R.; Strouse, C. E. *J. Am. Chem. Soc.* **1990**, *112*, 1865−1874.
(24) Byrn, M. P.; Curtis, C. J.; Goldberg, I.; Hsiou, Y.; Khan, S. I.; Sawin, P. A.; Tendick, S. K.; Strouse, C. E. *J. Am. Chem. Soc.* **1991**, *113*, 6549−6557.
(25) Byrn, M. P.; Curtis, C. J.; Hsiou, Y.; Khan, S. I.; Sawin, P. A.; Tendick, S. K.; Terzis, A.; Strouse, C. E. *J. Am. Chem. Soc.* **1993**, *115*, 9480−9497.
(26) Vogel, E.; Koch, P.; Hou, X.-L.; Lex, J.; Lausmann, M.; Kisters, M.; Aukauloo, M. A.; Richard, P.; Guilard, R. *Angew. Chem., Int. Ed. Engl.* **1993**, *32*, 1600−1604.
(27) Abbotto, A.; Alanzo, V.; Bradamante, S.; Pagani, G. A.; Rizzoli, C.; Calestani, G. *Gazz. Chim. Ital.* **1991**, *121*, 365−368.
(28) Alsfasser, R.; Vahrenkamp, H. *Chem. Ber.* **1993**, *126*, 695−701.
(29) Bremer, J.; Uhlenbrock, S.; Pinkerton, A. A.; Krebs, B. *Z. Anorg. Allg. Chem.* **1993**, *619*, 1183−1195.
(30) Hartmann, F.; Klaui, W.; Kremer-Aach, A.; Mootz, D.; Strerath, A.; Wunderlich, H. *Z. Anorg. Allg. Chem.* **1993**, *619*, 2071−2076.
(31) Lipkowski, J. *J. Coord. Chem.* **1990**, *22*, 153−158.
(32) Pickardt, J.; Gong, G.-T.; Wischnack, S.; Steinkopff, C. *Z. Naturforsch.* **1994**, *49b*, 325−329.
(33) Alcock, N. W.; Benniston, A. C.; Moore, P.; Pike, G. A.; Rawle, S. C. *J. Chem. Soc., Chem. Commun.* **1991**, 706−708.

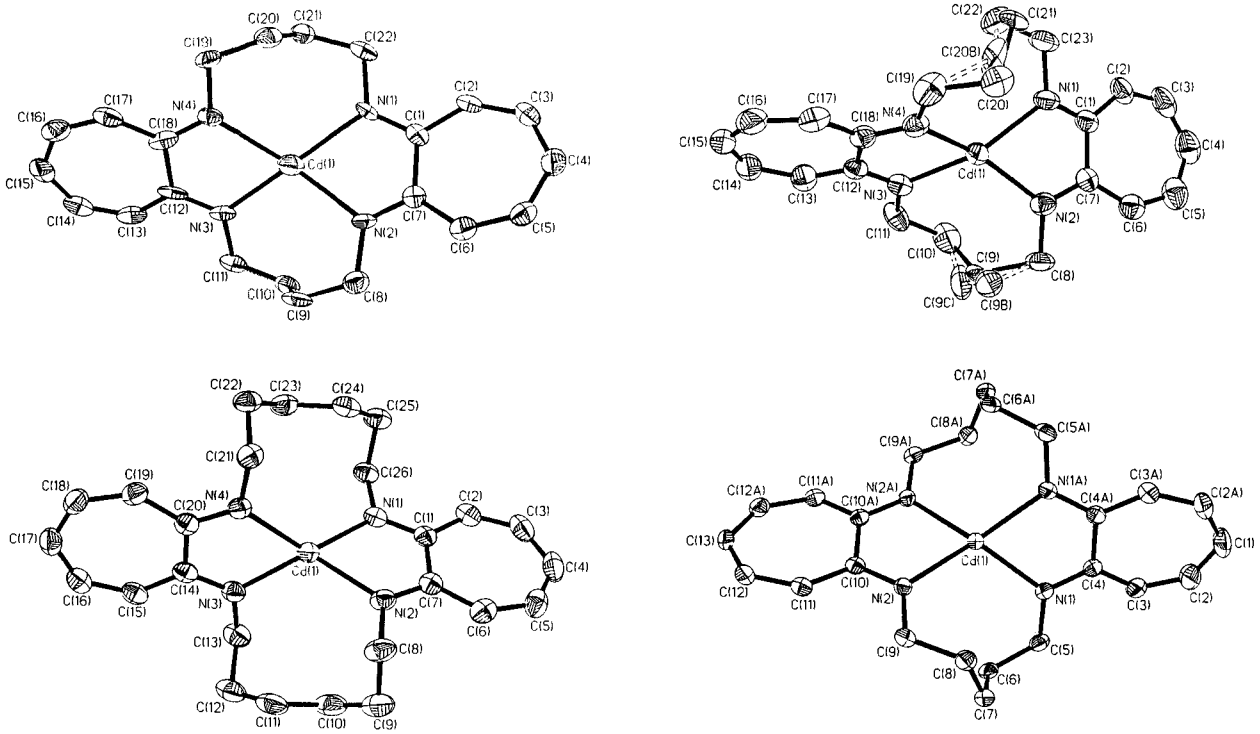

Figure 4. ORTEP diagrams with 50% thermal ellipsoids (clockwise from top left) [Cd(TC-4,4)], [Cd(TC-4,5)], [Cd(TC-5,5)], and [Cd(TC-6,6)]. The dashed lines in the depiction of [Cd(TC-4,5)] indicate the second orientation of the disordered polymethylene linker chains.

Table 5. Selected Bond Distances and Angles for Cadmium Tropocoronands[a]

	distances		angles	
[Cd(TC-4,4)]	Cd−N1	2.219(7)	N1−Cd−N2	71.9(3)
	Cd−N2	2.251(7)	N1−Cd−N3	165.6(3)
	Cd−N3	2.248(8)	N1−Cd−N4	111.8(3)
	Cd−N4	2.252(8)	N2−Cd−N3	111.6(3)
	Cd−N_{avg}	2.24(1)	N2−Cd−N4	152.9(3)
			N3−Cd−N4	71.8(3)
[Cd(TC-4,5)]	Cd−N1	2.209(5)	N1−Cd−N2	73.9(2)
	Cd−N2	2.193(6)	N1−Cd−N3	151.8(2)
	Cd−N3	2.202(6)	N1−Cd−N4	114.0(2)
	Cd−N4	2.195(6)	N2−Cd−N3	113.1(2)
	Cd−N_{avg}	2.200(6)	N2−Cd−N4	151.0(2)
			N3−Cd−N4	73.8(2)
[Cd(TC-5,5)]	Cd−N1	2.195(2)	N1−Cd−N1A	75.8(1)
	Cd−N2	2.197(2)	N1−Cd−N2	114.85(7)
	Cd−N_{avg}	2.196(1)	N1−Cd−N2A	147.51(7)
			N2−Cd−N2A	74.34(9)
[Cd(TC-6,6)]	Cd−N1	2.182(2)	N1−Cd−N2	73.99(9)
	Cd−N2	2.190(3)	N1−Cd−N3	134.32(9)
	Cd−N3	2.194(3)	N1−Cd−N4	127.15(8)
	Cd−N4	2.182(3)	N2−Cd−N3	122.03(8)
	Cd−N_{avg}	2.187(5)	N2−Cd−N4	134.45(9)
			N3−Cd−N4	74.16(9)

[a] Numbers in parentheses are estimated standard deviations of the last significant figure. Atoms are labeled as indicated in Figure 4.

angle greater than 9° has never been observed. The synthesis and structural characterization of [Zn(py)(TC-3,3)], in which zinc is displaced by 0.57 Å from the N_4 plane and the fold angle is 15°, further underscores the reason that a four-coordinate [Zn(TC-3,3)] complex cannot be made. The Zn(II) ion does not fit in the macrocycle hole, and the rigid TC-3,3 ligand cannot twist; it can only fold, upon coordination of a fifth ligand to accommodate the metal ion. Addition of one more methylene unit to the tropocoronand enlarges the macrocycle hole sufficiently to reduce the torsional strain in the linker chain, allowing the four-coordinate zinc complex, [Zn(TC-3,4)], to form. Here the Zn atom is still displaced from the N_4 plane,

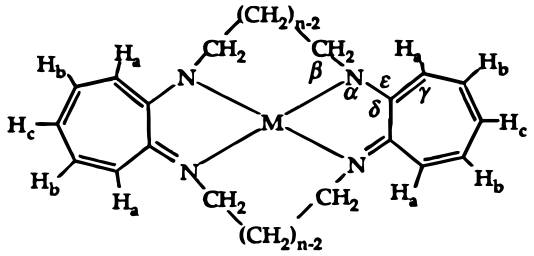

Figure 5. Labels for the tropocoronand complexes used in this paper.

but only by 0.015 Å, and the two seven-membered rings are twisted relative to one another at a dihedral angle of 36.4°. The torsion angles for the C9−C10 and C19−C20 bonds deviate from their predicted values by 22.6 and 49.8°, respectively, showing that substantial strain exists in these linker chains. The strained [Zn(TC-3,4)] complex, and our inability to prepare [Zn(TC-3,3)], demonstrate that the TC-3,4 macrocycle is the smallest tropocoronand ligand which will accommodate four-coordinate zinc.

The [Zn(TC-4,4)] complex is also four-coordinate, but the additional torsional strain in the linker chains forces the ligand to twist even further. Although this molecule has a five−seven−five−seven pattern of chelate rings, in contrast to the four six-membered chelate rings in metalloporphyrins, this difference is not the cause of the ligand twist. A square-planar Zn porphycene complex with a five−seven−five−seven chelate

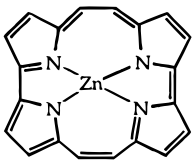

zinc porphycene

ring set has been characterized in which the Zn atom is displaced from the N_4 plane by only 0.05 Å.[26] In the porphycene ligand,

the carbon atoms all have sp^2 hybridization, leading to a completely conjugated macrocycle which enforces planarity. The saturated polymethylene linker chains in [Zn(TC-4,4)] generate a larger macrocyclic hole, reflecting ligand twist. Contraction of the "circumference" of a macrocycle upon oxidation has been observed in other systems.[34]

The Θ values for the remaining [Zn(TC-4,5)], [Zn(TC-5,5)], and [Zn(TC-6,6)] complexes are very similar to those for the other first-row [M(TC-*n*,*m*)] tropocoronands listed in Table 4. These expanded macrocycles bind much larger metal ions, such as cadmium ($r = 0.92$ Å), without substantial strain and do not reflect the subtle changes in ionic radii from Co(II) to Zn(II). Larger changes in metal ion radii produce significant geometric consequences, however, as discussed below.

The [Zn(py)(TC-3,3)] complex is the first example where a divalent, first-row metal ion did not form a square-planar complex with the TC-3,3 ligand. Several related square-pyramidal $Zn(py)N_4$ complexes have been structurally characterized. Included are five-coordinate [Zn(py)porph] complexes, in which the average displacement of zinc from the N_4 plane is 0.31−0.37 Å, smaller than the 0.57 Å value in [Zn(py)(TC-3,3)]. The Zn−pyridine distances in the [Zn(py)porph] complexes range from 2.15 to 2.20 Å,[35] compared to 2.096(4) Å in [Zn(py)(TC-3,3)]. These differences are a consequence of the macrocycle hole size which is larger in the 16-membered porphyrins than in the 14-membered TC-3,3 ring. The larger macrocycle hole in porphyrin complexes affords weaker coordination of the axial base, a smaller displacement of zinc out of the N_4 plane, and longer Zn−pyridine bond distances. The average $Zn-N_{TC}$ distance of 2.055(5) Å reflects stronger electron donation from the TC ligand than from the porphyrin to zinc in [Zn(py)porph] complexes, where the average $Zn-N_{pyrrole}$ distance is 2.06−2.08 Å.[35]

Two other macrocyclic $[Zn(base)N_4]$ complexes, $[Zn(NR_3)$(tmtaa)], where tmtaa = the dibenzotetramethylaza[14]annulene dianion and R = Et and *n*-Pr, have been prepared.[36] Like TC-3,3, tmtaa is a 14-membered macrocycle with a five−six−five−six chelate ring pattern and planar nitrogen atoms. The $[Zn(NR_3)$(tmtaa)] complexes were not structurally characterized but were assigned a square pyramidal geometry on the basis of molecular modeling and ^{1}H NMR spectroscopic studies. The four methyl groups of the tmtaa ligand would clash sterically with the phenyl ring ortho protons if the macrocycle were bent into a saddle conformation forcing the phenyl rings up and the methyl groups down.[37] The tmtaa ligand is apparently too small to accommodate Zn(II) in the plane of the macrocycle, and the fact that no [Zn(tmtaa)] complexes could be isolated parallels our results with the TC-3,3 tropocoronand.

[Cd(TC-*n*,*m*)] Complexes. Cadmium(II), like zinc(II), has no electronically preferred geometries. Most Cd(II) complexes are six-coordinate and not four-coordinate. A recent search of the Cambridge Structural Database[38] found 184 complexes of cadmium coordinated to four nitrogen donors, but only nine of the complexes were four-coordinate. The larger Cd(II) ionic radius, 0.92 Å versus 0.74 Å for Zn(II),[7] readily accommodates two or more additional ligands. The only previously reported macrocyclic CdN_4 species are porphyrins investigated in the solid state as clathrate hosts.[24] These complexes are rigorously square planar, and no nonplanar macrocyclic complexes of Cd have been reported, although a few acyclic tetrahedral CdN_4 species exist.[39−41] No macrocyclic complexes with geometries intermediate between square planar and tetrahedral have been observed.

Table 6. Zinc and Cadmium Tropcoronand α-to-ω Distances (Å)[a]

zinc			cadmium		
	α−ω (Å)			α−ω (Å)	
complex	chain no. 1	chain no. 2	complex	chain no. 1	chain no. 2
[Zn(TC-3,4)]	2.56	3.70			
[Zn(TC-4,4)]	3.17	3.71	[Cd(TC-4,4)]	3.78	3.77
[Zn(TC-4,5)][b]	3.21	4.18	[Cd(TC-4,5)]	4.07	4.02
[Zn(TC-5,5)]	4.13	4.13	[Cd(TC-5,5)]	4.26	4.26
[Zn(TC-6,6)]	4.51	4.48	[Cd(TC-6,6)]	4.63	4.73

[a] Defined as indicated in the following diagram:

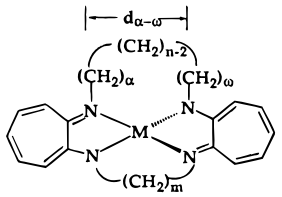

[b] Average from two crystallographically independent molecules.

The ability of the tropocoronand ligand to tune the geometric properties and stabilize unusual metal coordination spheres is nicely manifest in the cadmium series. The pseudo-tetrahedral [Cd(TC-*n*,*m*)] complexes all have smaller dihedral angles than the [Zn(TC-*n*,*m*)] homologues, as shown in Table 4 and Figure 2. The larger ionic radius of Cd(II) increases the Cd−N over the Zn−N bond lengths, leading to increases in the α-to-ω separation (Table 6), which directly affects Θ. As the α-to-ω distance increases, torsional strain is relieved in the macrocycle and therefore less twist, as measured by Θ, is required to minimize linker chain distortions for the same size macrocycle. Thus the [Cd(TC-*n*,*m*)] complexes have smaller twist angles than their zinc analogs. The average α-to-ω distance increases (Table 6) from 4.13 Å in [Zn(TC-5,5)] to 4.26 Å in [Cd(TC-5,5)], and Θ decreases by 15.3°. For [Zn(TC-6,6)] and [Cd(TC-6,6)] the same distance increases from 4.50 to 4.68 Å and Θ is 5.6° smaller. In the TC-4,4 complexes, extension of the distance from 3.44 Å for Zn(II) to 3.78 Å with Cd(II) reduces Θ, resulting in the small, saddle-type fold of the macrocycle by 9.8° needed for [Cd(TC-4,4)].

The only [Cd(TC-*n*,*m*)] complex that is closer to square planar than tetrahedral is [Cd(TC-4,4)]. Figure 2 shows a monotonic trend in Θ for $n + m = 9$, 10, and 12 which, if extrapolated to the $n + m = 8$ point, would require a twist angle of approximately 40° for [Cd(TC-4,4)]. The ORTEP diagram for this complex (Figure 4) shows that the ligand is twisted, but a detailed inspection of the structure reveals that it is also folded. The angle formed by Cd and the two γ ring carbon atoms (attached to H_c, Figure 5), C4−Cd−C15, is 170.2°, meaning that the dihedral angle between the two aminotroponiminate rings is a consequence of both twisting and folding. Thus [Cd(TC-4,4)] was not included in the plot of Θ versus $(n + m)$ in Figure 2, which describes only the twist component.

The folding of the ligand in [Cd(TC-4,4)] also results in displacement of the metal by 0.124 Å from the N_4 plane. This

(34) Hancock, R. D.; Martell, A. E. *Chem. Rev.* **1989**, *89*, 1875−1914.
(35) Anderson, H. L.; Bashall, A.; Henrick, K.; McPartlin, M.; Sanders, J. K. M. *Angew. Chem., Int. Ed. Engl.* **1994**, *33*, 429−431.
(36) Neves, D. R.; Dabrowiak, J. C. *Inorg. Chem.* **1976**, *15*, 129−134.
(37) Cotton, F. A.; Czuchajowska, J. *Polyhedron* **1990**, *9*, 2553−2566.
(38) Allen, F. H.; Davies, J. E.; Galloy, J. J.; Johnson, O.; Kennard, O.; Macrae, C. F.; Mitchell, E. M.; Mitchell, G. F.; Smith, J. M.; Watson, D. G. *J. Chem. Info. Comput. Sci.* **1991**, *31*, 187−204.
(39) Barr, D.; Edwards, A. J.; Raithby, P. R.; Rennie, M.-A.; Verhorevoort, K.; Wright, D. S. *J. Chem. Soc., Chem. Commun.* **1994**, 1627−1628.
(40) Menabue, L.; Saladini, M. *J. Inorg. Biochem.* **1993**, *49*, 201−207.
(41) Wirringa, U.; Roesky, H. W.; Noltemeyer, M.; Schmidt, H.-G. *Angew. Chem., Int. Ed. Engl.* **1993**, *32*, 1628−1630.

Table 7. Displacement (Å) of M(II) from Best N_4 Plane in [M(TC-*n*,*m*)] Complexes

$n + m$	Co[a] (0.72 Å)[b]	Ni[c] (0.69 Å)	Cu[d] (0.71 Å)	Zn (0.74 Å)	Cd (0.92 Å)
6	0.09	0.101	0.0	*e*	*e*
7	*f*	*f*	*f*	0.015	*e*
8	0.017	0.012	0.021	0.085	0.124
9	0.115	0.049	f	0.004	0.006
10	0.0	0.0	0.0	0.0	0.0
12	0.038	0.063	*e*	0.043	0.001

[a] Reference 6. [b] Ionic radius, ref 7. [c] Reference 4. [d] Reference 5. [e] Complex not accessible. [f] Structure not determined.

result strongly suggests that species containing the [Cd(TC-3,3)] or [Cd(TC-3,4)] moiety would exist if Cd were more significantly displaced from the N_4 plane. Such a structure would be stabilized by coordination of additional ligands, as occurs in five-coordinate [Zn(py)(TC-3,3)] and the known six-coordinate [ZrX_2(TC-3,3)] species.[18] Pseudo-square-planar [Cd(TC-4,4)] is an important molecule because it demonstrates that ligand twist is not the only mode of flexibility available to the tropocoronand macrocycle and that twisting is not always required to relieve torsional strain.

The [Cd(TC-4,5)] complex (Figure 4) has a dihedral angle of 48.5°, almost exactly halfway between square planar, $\Theta = 0°$, and tetrahedral, $\Theta = 90°$, geometries; this angle is an average of two values, owing to the positional disorder of the ligand. The [Cd(TC-5,5)] and [Cd(TC-6,6)] complexes have fold angles of 0.0 and 0.8°, respectively, consistent with less displacement of the cadmium center out of the N_4 plane (Table 7) and less folding.

An important consequence of this analysis is that the dihedral angle Θ between aminotroponiminate rings comprises both twist and fold components. Their relative contributions can be visually discerned and quantitatively distinguished by changes in the α-to-ω distances as a function of increasing dihedral angle with reference to a perfectly planar ligand. In a purely twisting motion, the aminotroponiminate rings rotate in opposite directions, increasing the α-to-ω distance and making the nitrogen atoms nonplanar. When the ligand folds, the seven-membered rings bend toward each other, decreasing the α-to-ω distance and maintaining the N_4 square plane. These individual components are shown schematically in Figure 6.

Structural Trends in M(TC-*n*,*m*)] Complexes. Table 7 shows the distance from the metal ion to the best N_4 plane for all the structurally characterized [M(TC-*n*,*m*)] complexes. This displacement is never greater than 0.124 Å, and larger displacements are observed only in the presence of a fifth ligand, e.g. [Zn(py)(TC-3,3)]. The 0.0 Å displacements observed for the [M(TC-5,5)] complexes reflect the fact that they all have a crystallographically imposed 2-fold axis passing through the metal center.

The Zn−N_{avg} and Cd−N_{avg} distances decrease with increasing dihedral angle (Tables 3 and 4), a trend opposite to that observed in the Co(II), Ni(II), and Cu(II) complexes. Insight into this difference is afforded by results for the related acyclic [M(R_2-ati)$_2$] complexes, the M−N_{avg} distances of which are taken as unconstrained for this type of metal−ligand bond. For example, in the [Cu(TC-*n*,*m*)] complexes, the Cu−N_{avg} distance increases from 1.939(6) to 1.96(1) Å for $n = m = 3$ to 5,[5] whereas the average Cu−N distance in [Cu(Ph_2ati)$_2$] is 1.937(5) Å.[19,20] This difference reflects the fact that the torsional demands of the larger macrocycles are incompatible with the small radius of Cu(II). The smaller [Cu(TC-*n*,*m*)] complexes have Cu−N bond lengths closer to the unconstrained values.

The Zn−N_{avg} distance in the acyclic complex [Zn(Ph_2ati)$_2$] is 1.98(1) Å,[19,20] which most closely matches the Zn−N_{avg} distance of 1.981(3) Å in [Zn(TC-6,6)]. This result indicates that the Zn−N distances are closer to their ideal values in larger macrocycles rather than in smaller ones, unlike the Cu series. Therefore a trend of M−N distances away from the ideal, unconstrained value is taken as an indicator of a poorer fit of the metal ion into the macrocycle. Cu(II) fits better into TC-3,3, and Zn(II) fits better into TC-6,6. No ati complexes of Cd(II) are available, but the trends in dihedral angles suggest that this metal ion would favor larger tropocoronand macrocycles.

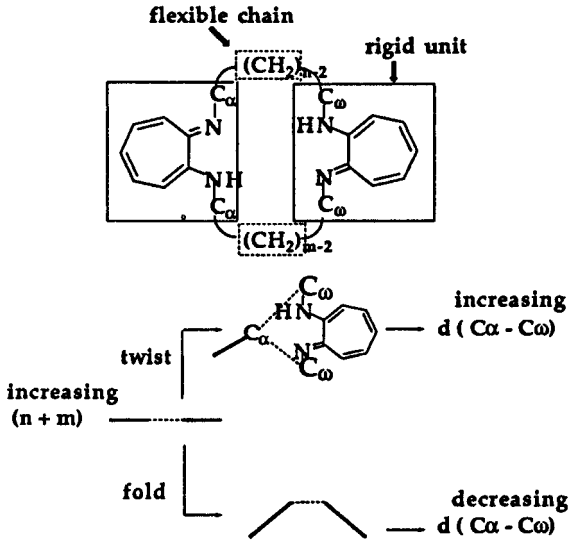

Figure 6. Tropocoronand twisting and folding components. In the top diagram the rectangles enclose the rigid parts of the ligand, all atoms of which are required to be coplanar. The twist motion represents rotation of the two rectangles about an axis joining the outermost carbon atoms of the seven-membered rings and increases the $C_\alpha-C_\omega$ distance. The fold motion represents movement of the two rectangles toward one another such that the distance between the outermost carbon atoms of the seven-membered rings and the $C_\alpha-C_\omega$ distance both decrease.

In addition to the decrease in Θ and increase in M−N bond lengths in Cd(II) versus Zn(II) for the same ligand, the average value of the M−N−C angle α increases from 115.6(8)° in the zinc(II) complexes to 117(1)° for those of cadmium(II) and the average M−N−CH_2 angle β decreases from 123(1) to 121(1)° upon changing from Zn(II) to Cd(II). Both trends are consistent with the larger Cd(II) ion forcing a wider angle within the five-membered chelate ring at the expense of the angle at the first linker chain methylene group. The remaining internal tropocoronand ligand parameters are quite consistent within and between members of the two series of complexes.

The chelate rings involving the polymethylene linker chains can potentially assume many different conformations, some more energetically favored than others. The α-to-ω distance in these aliphatic chelate rings is the primary source of linker chain torsional strain, and these distances in the zinc(II) and cadmium(II) tropocoronands are reported in Table 6. The α-to-ω distance in a particular [M(TC-*n*,*m*)] complex may require the chelate ring to adopt a conformation that is more strained than in a complex with a different α-to-ω distance. A recent study of Co(III) complexes with six-membered diamine chelate rings demonstrated that high-energy conformations occurred when ligand steric restrictions prevented adoption of the energetically most favored conformer.[42] Increasing Θ in [M(TC-*n*,*m*)], M = Co, Ni, and Cu, increases the α-to-ω distance and decreases torsional strain in the linker chains. It

(42) DaCruz, M. F.; Zimmer, M. *Inorg. Chem.* **1996**, *35*, 2872−2877.
(43) Collins, T. J. *Acc. Chem. Res.* **1994**, *27*, 279−285.

was therefore anticipated that, for a particular macrocycle with Zn and Cd, the complex with the longer α-to-ω distance would show the least linker chain distortion. The structural data in Tables 5, 7, and 8 do not consistently support this hypothesis, however. The α-to-ω distance in [Cd(TC-6,6)] is 0.18 Å greater than in [Zn(TC-6,6)] and the average Cd torsion angles are smaller by 4°, as expected. In contrast, the α-to-ω distance in [Zn(TC-5,5)] is 0.13 Å smaller than in [Cd(TC-5,5)], but the average distortion in the linker chains is 5° *less* in the C−C bonds and 19° *less* in the C−N bonds of [Zn(TC-5,5)] compared to [Cd(TC-5,5)]. Thus a metal ion with a significantly larger radius experiences increased torsional strain in tropocoronands having smaller α-to-ω distances because their size is better accommodated by greater distances and larger macrocycle holes.

Cyclic Voltammetry. Cyclic voltammetric studies of the [Zn(TC-*n*,*m*)] complexes revealed ligand redox behavior in accord with their known reactivity. The ligand is highly resistant to reduction, consistent with its stability in the 40% Na/Hg solutions used to generate Na[Co(TC-*n*,*m*)] species.[17] The irreversible oxidation waves observed at 0.5 V vs ferrocenium/ferrocene in CH_2Cl_2 may reflect decomposition involving the linker chains. Macrocycles with C−H bonds adjacent to nitrogen atoms are sometimes incompatible with highly oxidized metal centers.[43] Metal ion attack of the linker chains has been observed in some organometallic Zr(IV) and Hf(IV) tropocoronand complexes,[18] and it is reasonable to suppose that other oxidants might similarly react with the linker chains. The use of tropocoronand macrocycles to stabilize transition metals in unusually high oxidation states may require more robust linker chain groups than polymethylene chains.

Conclusions

The mononuclear zinc(II) tropocoronands [Zn(TC-*n*,*m*)], $n + m = 7, 8, 9, 10, 12$, have afforded considerable insight into this class of coordination compound. The inability to obtain [Zn(TC-3,3)], the synthesis of [Zn(py)(TC-3,3)], and the structural analysis of [Zn(TC-3,4)] suggest that the relatively large Zn(II) ion prohibits formation of four-coordinate Zn(II) with a 14-membered tetraazamacrocycle of this kind. Structures of the larger zinc tropocoronands exhibit significantly larger dihedral angles compared with their copper analogs. The monotonic changes of the twist angle Θ with increasing $n + m$ in the [Zn(TC-*n*,*m*)] complexes contrast with the behavior of related Co(II) and Ni(II) complexes, consistent with the absence of spin-state changes for Zn(II).

The [Cd(TC-*n*,*m*)] complexes, $n + m = 8, 9, 10$, and 12, have dihedral angles Θ smaller than those of their Zn congeners. This result demonstrates that the increase in M−N distance with a larger metal diminishes Θ because of the increased α-to-ω distances. Displacement of Cd out of the N_4 plane in [Cd(TC-4,4)] afforded a saddle-type fold not previously encountered in [M(TC-*n*,*m*)] complexes. The dihedral angle between the aminotroponiminate rings in [M(TC-*n*,*m*)] complexes has both fold and twist components which differ in their effect on the α-to-ω linker chain distance.

Cyclic voltammetric studies of [Zn(TC-*n*,*m*)] complexes demonstrated stability of the ligand to strongly reducing potentials, but an irreversible oxidation occurred at moderately oxidizing potentials.

Acknowledgment. This work was supported by a grant from the National Science Foundation. We thank Drs. Maria Bautista, Mike Scott, and Peter Fuhrmann for assistance and comments on the manuscript.

Supporting Information Available: Tables S1−S42 listing atomic coordinates and B_{eq} values, anisotropic thermal parameters, intramolecular bond distances and angles, and ligand linker chain torsion angles for the zinc and cadmium tropocoronand complexes, and Figure S1, displaying cyclic voltammograms of [Zn(TC-4,4)] in CH_2Cl_2 and THF (59 pages). Ordering information is given on any current masthead page.

IC970033O